Evolution, Geodynamics, and Morphology of Lenticular Extension Zones of Transform Faults: Comparative Analysis and Kinematic Model

K. O. Dobrolyubova*

Geological Institute, Russian Academy of Sciences, Moscow, 119017 Russia
*e-mail: k_dobrolubova@mail.ru
Received October 10, 2024; revised March 13, 2025; accepted March 27, 2025

Abstract—The article presents a new type of morphostructural objects defined by the author: intratransform lenticular extensions confined to active troughs of transform faults. A morphostructural analysis is carried out using geophysical data. It has been revealed that such structures are formed in active zones of transform faults with maximum offset of segments of the mid-ocean ridge. Intratransform lenticular extension zones have been classified, according to which types I—III of morphostructures were identified, which illustrate not only various evolutionary stages, but also various kinematic scenarios. Type I is a lenticular zone. This type includes small, young (<10 Ma) lenticular extension zones of the local level, occurring mainly in the transform fault of the Southern Hemisphere. Type II is a lenticular transformed basin. It is a lenticular formation at the regional level with a large (~100 to ~300 km) offset formed on a large transform fault with a block of highly deformed lithosphere in the axial part of the lens and shear movements along one of their fringing arc troughs, but without internal spreading segments. Type III is a multitransform lenticular system. This is a global level lenticular formation, located on a large transform boundary with an extreme offset, limited by passive arcuate scarps and enclosed between them by several closely spaced transform fault trough valleys and internal spreading zones. A kinematic model is constructed for identified morphostructure types I—III in accordance with the classification of intratransform lenticular extension zones.

Keywords: spreading, transform fault, geomorphology, transform fault tectonics, active part of transform fault, accretion, seismicity, gravity anomalies, kinematic model

DOI: 10.1134/S0016852125700141

INTRODUCTION

The patterns of the origin and evolution of oceanic crust, rift segments, and transform faults that displace them, which are the main elements of oceanic crust, have been substantiated by the of plates tectonics theory. Recently, studies have carried out that significantly complement and complicate the scenarios of tectonic processes [18, 20, 21]. The structure of transform fault troughs is of interest for research [9, 15, 16, 19, 20, 26–29].

Tomography data confirm that beneath the midocean ridge (MOR) system at depths greater than 200–300 km, no single region of heated mantle with ascent from its base has been recorded [17]. This confirms the hypothesis that spreading is secondary and is a compensatory response to lithospheric plate movement, substantiated in the 1990s [23, 34].

The assumption that extension zones arising in the most zones of weakness are filled with new crust, which allows us to explain its formation not only along a divergent, but also along a transform boundary. This may key to understanding the formation of the com-

plex morphology of transform fault troughs and intralenticular zones that complicate the troughs of some transform faults.

Studies in the deep-water Atlantic and other oceans have shown the presence of neotectonic movements and degassing in the passive parts of transform faults and at the boundaries of segments of different ages [20].

The boundaries of these segments, represented by megatransform systems and faults with a large offset of the MOR axis, represent a special structure with contrasting geophysical properties and an atypical morphology of the basaltic basement. They separate segments of basins with different durations of thermal history, in which there exists the possibility of neotectonic displacements, both in the active parts of faults and near the MOR, and in the reactivated passive parts of faults at large distances from the MOR [4, 6, 13, 14, 20].

The aim of this article is to study atypical morphostructures, which are lenticular extensions of transform fault troughs. The large volume of data confirming the widespread distribution of these objects makes

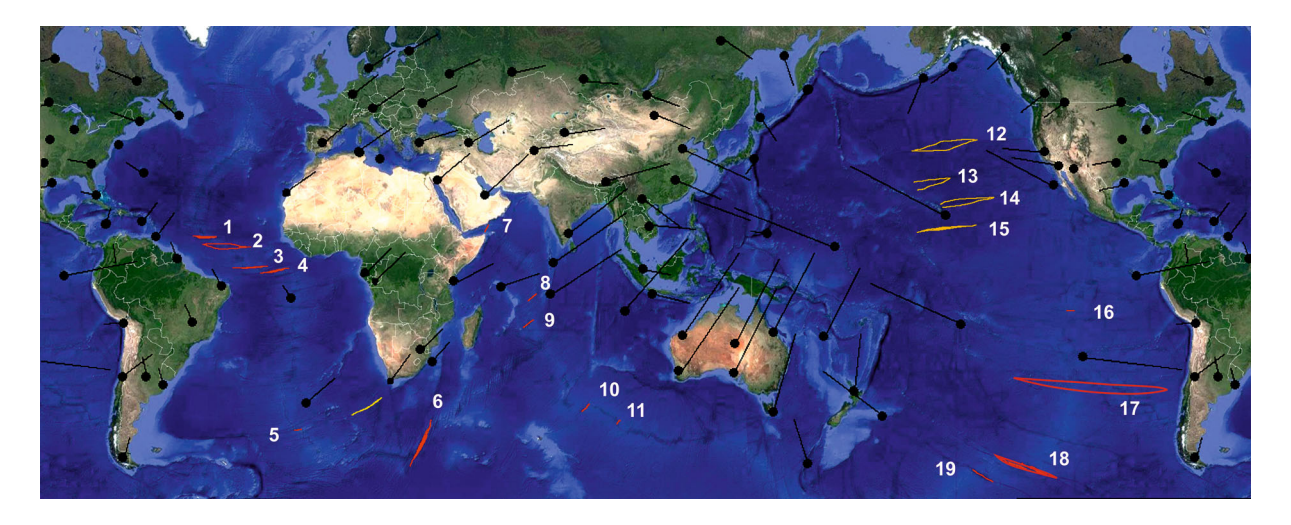


Fig. 1. Distribution of lenticular extensions of transform fault valleys in the World Ocean and vectors of continental movement (according to data from [35, 36]). Lines show lenticular extensions: active (red); relict (yellow). Vectors of movement of lithospheric plates at measurement reference points according to GPS data are indicated (black arrow, size of arrow is proportional to speed of movement). Abbreviations: TF, transform fault; MTLS, multitransform lenticular system. Arabic numerals on map show 1, Vema TF; 2, Doldrums MTLS; 3, São Paulo MTLS; 4, Romanche TF; 5, Agulhas TF; 6, Andrew-Bain TF; 7, Alula-Fartak TF; 8, Vema Trough; 9, Marie Celeste TF; 10, 88 °E TF; 11; 96° E TF; 12, Mendocino TF; 13, Murray TF; 14, Molokai TF; 15, Clarion TF; 16, Garrett TF; 17, Valdivia MTLS; 18, Eltanin MTLS; 19, Udintseva MTLS.

it possible to identify a number of patterns and trace the development of these structures.

LENTICULAR EXTENSIONS OF THE MID-ATLANTIC RIDGE ZONE

Lenticular extensions are lens-shaped, in plan view, expansions of transform fault valleys, formed by one or several subparallel narrow trough valleys that are well expressed in the relief, alternating with intertrough ridges. Lenticular extensions are limited distinct arcuate scarps in plan view and are most often located within the active part of a transform fault between two spreading centers.

M. Ligi et al. [29] made one of the first hypotheses explaining the emergence of a lenticular extension of a transform fault, based on the results of joint Russian—Italian research in the Equatorial Atlantic from 1985 to 1998. According to this hypothesis, such objects arise in transform faults under conditions of significant offset (at least 100 km) between two active spreading centers. Due to the large temperature contrast between noncoeval lithospheric plates, which are in contact along a fault, in the active part of a transform fault the formation of two arcuate shifts in plan is possible, associated with two zones of reduced strength of the lithosphere, along which the adjacent plates move in different directions [29].

Under conditions of significant uncompensated local tension across the structure, conditions arise for the formation of a median ridge between the strikeslip walls. Over time, the zone expands and takes on the appearance of a lenticular extension with multiple

subparallel transform fault troughs and ridges separating them [29].

Lenticular zones are found not only at the regional and local levels, as parts of single transform faults; they can also be complex formations of a global planetary level, consisting of large transform faults.

We propose that these lenticular systems are more evolutionarily mature structures formed from simple lenticular extensions. The distribution pattern of lenticular extensions identified from bathymetric survey data shows active and relict lenticular extensions, as well as plate movement vectors [36, 38] (Fig. 1).

Lenticular extensions (Fig. 1) are either grouped together to form series of en echenlon—like subparallel lenses (type I), or they are single structures, found primarily in the Southern Hemisphere (type II).

Type I includes two groups:

— active in the Equatorial Atlantic Ocean, including the Romanche, São Paulo, Doldrums, and Vema faults:

— relict, located in the Pacific Ocean on the flanks of the Mendocino, Murray, and Molokai faults.

Taking into account movement of the Pacific Plate established by GPS data [36], as well as dating of magnetic anomalies, it can be suggested that the Pacific group of lenticular extensions was active and located in the equatorial region; however, over time, it ceased to develop, but as a relict, the morphostructure continues to move northwest along with the flanks of the Pacific Plate.

Single lenticular extensions are located predominantly in the Southern Hemisphere. Among them are both forms with a large offset, the formation of which

can be explained by the hypothesis of M. Ligi et al. [29], and small forms with an insignificant offset, the formation of which this hypothesis does not explain.

M. Ligi et al., as well as a number of domestic specialists, classify large lens-shaped extensions such as Romanche, Doldrums, Sao Paulo and Andrew Bain as megatransforms [27, 29] and megatransform systems, which they identified as a special type of interplate boundaries [15].

MATERIALS AND METHODS

The study used data from a multibeam bathymetric survey obtained during expeditions conducted by the Geological Institute, Russian Academy of Sciences (GIN RAS, Moscow, Russia) in 1985–2019 on the R/V *Akademik Nikolaj Strakhov* in the Equatorial and South Atlantic.

Based on the obtained primary data, digital elevation models (DEMs) with a grid cell of 200 m were constructed. As a background coverage in places where there is no data for a detailed bathymetric survey, a 15 s GEBCO grid was used [35].

DEMs were calculated and constructed in the Surfer-19 [39] program. Morphometric measurements and construction of cross-section profiles were done in the Global Mapper program [40]. Additional data from geophysical coverages using the ARC-GIS software package [41]. To determine the age of geodynamic restructurings, we used a map of ages of the acoustic basement, calculated on the basis of anomalous magnetic field data.

Compilation of geophysical and bathymetric GEBCO [35], USGS [37], GPS Time Series Data [36], as well as data obtained on GIN RAS expeditions in 1985–2019, made it possible to take a new look at the morphology and evolution of the active parts of transform faults.

DATA PROCESSING AND INTERPRETATION

Active lenticular objects formed in transform fault troughs are grouped by morphology into three types, corresponding to different levels and stages of structure formation:

- lenticular zone (type I);
- lenticular transformed basin (type II);
- multitransform lenticular system (type III).

Lenticular Zone

Type I includes small lenticular extensions of the local level, which are the youngest structural formations and have the widest distribution in the World Ocean. Type I lenticular dilatations are found almost everywhere in the Southern Hemisphere and are most widely represented in the Indian Ocean.

Agulhas transform fault. In the South Atlantic, in the active zone of the Agulhas transform fault, a single lenticular extension has been recorded (Fig. 2).

The Agulhas Trough is a narrow, long depression clearly marked in the relief, up to 12 km wide, 225 km long, with a maximum depth of 5502 m. In the central part of the trough, the depth exceeds 2 km with respect to its walls. The length-to-width ratio is 18.7 and is the narrowest known lens. The lenticular extension occupies almost the entire active part of the Agulhas transform fault; the fault is characterized by a large offset, from the point of the Bouvet triple junction to the fault located at 35° S.

The floor of the valley of the transform fault trough in the central, deepest parts are flat and filled with sedimentary deposits. Near the eastern and western intersections, the sedimentary cover is insignificant in thickness and does not cover the bedrock.

In the central and eastern parts of the valley, the median ridge is clearly visible—elongated, narrow, straightened, without displacements or breaks (Fig. 2b). The height of the ridge is 150–200 m; the width is 1.5 km.

The marginal scarps of the lenticular extension are quest-like; the northern scarp is steeper and has a larger amplitude. The margins of the lenticular extension are limited by intersections. Nodal depressions are not expressed in the relief.

The analysis of the data on the age of the acoustic basement and bathymetric data makes it possible to suggest that the active opening of the lens occurred no earlier than 4 Ma, but within 2 Ma, the situation stabilized and the transverse expansion ceased or significantly decreased. This time marks the powerful riftogenic uplift in the area of the eastern intersect.

In the Indian Ocean, according to GEBCO data [35], five type I lenticular extensions have been identified, but detailed bathymetric data are available only for two of them (see Fig. 1).

Transform fault at 88° E. In In the active part of the transform fault in the vicinity of 88° E, a detailed bathymetric survey mapped a lenticular extension, the offset of which is 70 km, the length is 64 km, and the maximum width in the central part of 6 km. The length-to-width ratio is 10.6. The maximum depth is 4192 m. The depth of the bottom relative to the margins in the central part exceeds 1500 m (Fig. 3).

The offset of the 88° E fault is not the largest amplitude in the area; on the contrary, it is located 240 km east of a large transform fault with an offset of ~300 km.

The floor of the fault trough is leveled and probably filled with sediments. The transverse profile is trough-shaped (Fig. 3).

No clear median ridges were found. The marginal scarps are quest-like; the northwestern scarp is more dramatic and steep. The margins of the lens are limited by intersects. Nodal depressions are not recorded.

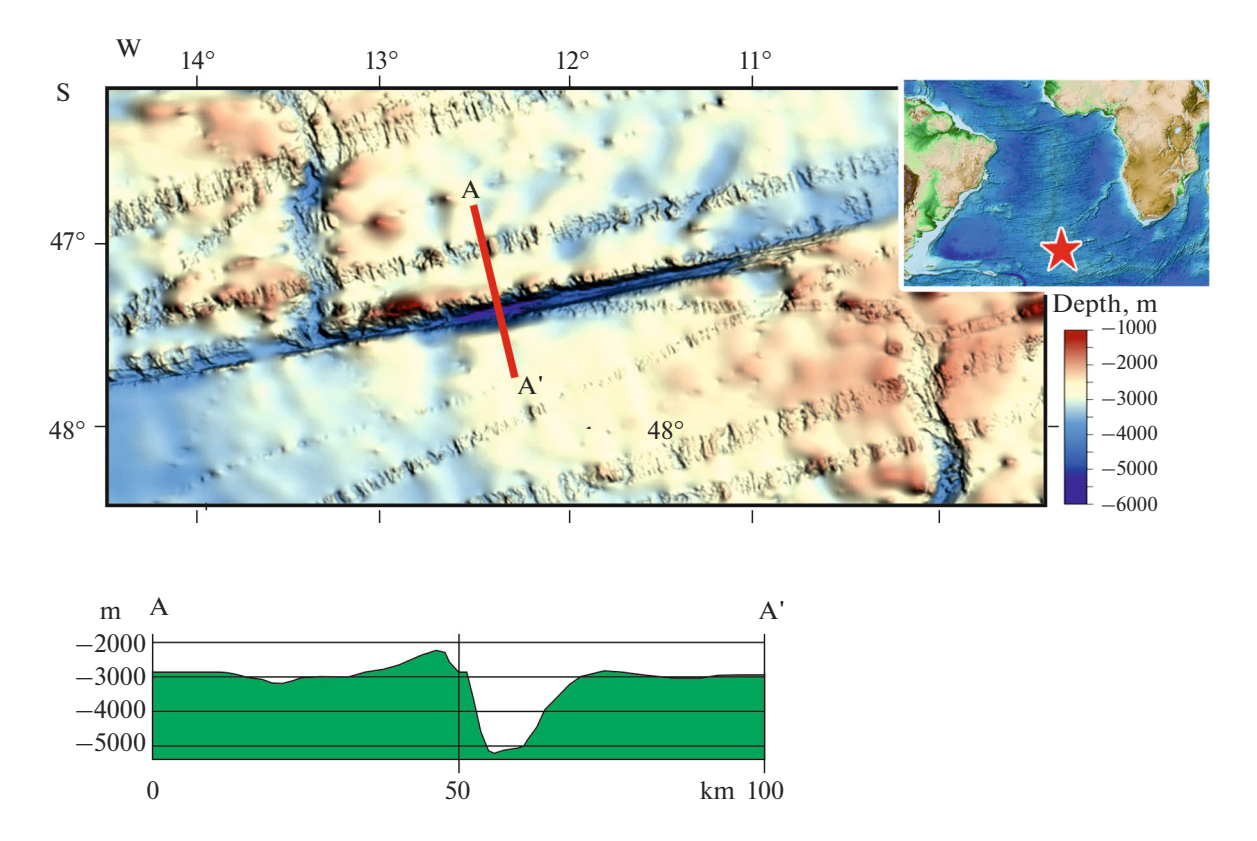


Fig. 2. Lenticular extension in active part of Agulhas transform fault (according to [35]). Transverse profile A—A' in entral part of lenticular extension is shown. Inset: location of object (red asterisk).

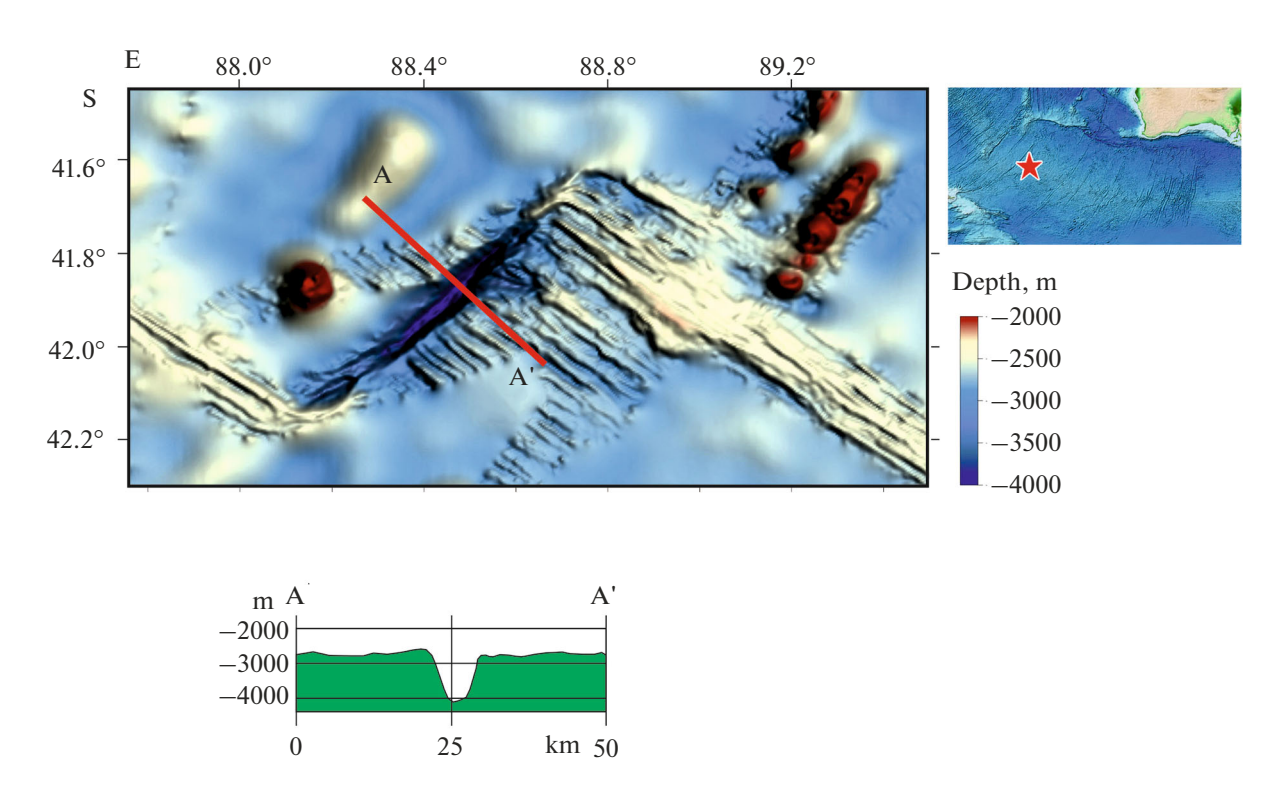


Fig. 3. Lenticular extension in active part of 88° E transform fault (according to [35]). Transverse profile A–A' in central part of lenticular extension is shown. On map (right): location of object (red asterisk).

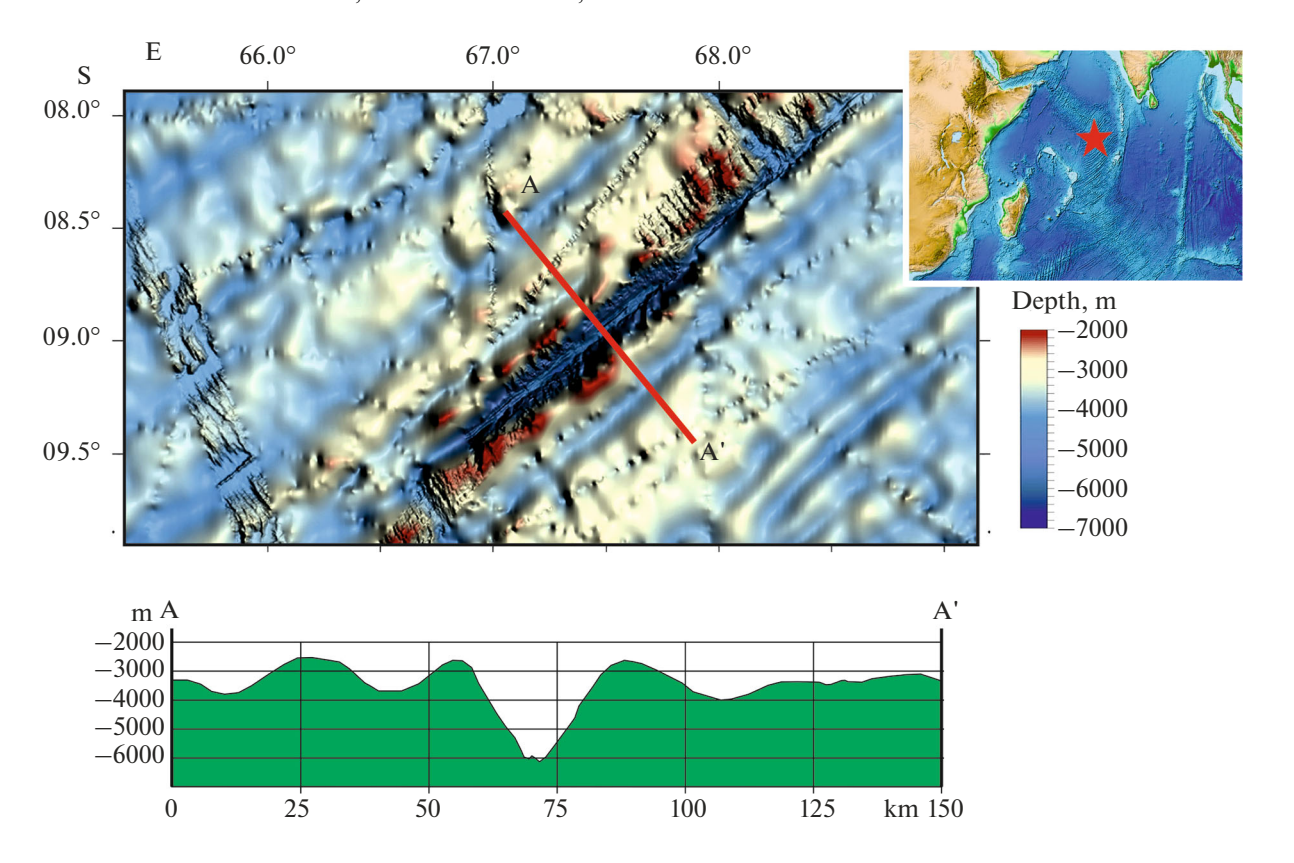


Fig. 4. Lenticular extension in active part of Vema transform fault in Indian Ocean (according to [35]). Transverse profile A–A' in central part of lenticular extension is shown. Inset: location of object (red asterisk).

According to GEBCO [35], in the Central Indian Ridge, three forms have been clearly identified that can be characterized as lenticular extensions, but detailed bathymetric surveys have only been carried out in the Vema Trough, located at coordinates 9° S, 67.5° E. The Vema Trough in active parts is a distinct narrow, long, lenticular depression with a maximum width of 24 km, length of 235 km, and depth of 6560 m (Fig. 4).

The length-to-width ratio is 9.8. The cross section is V-shaped. The depth of the bottom relative to the margins in the central part reaches 3300 m. The bottom is narrow, with almost no sedimentary cover. The marginal scarps are quest-like; no asymmetry of the scarps has been identified (Fig. 4).

In the axial part of the valley, a fragmentary median ridge has been mapped, the height of which does not exceed 150 m with a width of ~2 km. The lens peaks coincide with the intersects; nodal depressions have not been recorded. The age of the lenticular extension is estimated to be no older than 10 Ma.

Garrett transform fault. In the Pacific Ocean, one type I lenticular extension was identified, located in the region of 13° S in the active part of the Garrett transform fault. The Garrett rift trough in the active part has significantly widened and has a lenticular form with a maximum width of 19.7 km, length of 125 km, and

depth of 5102 m. The length-to-width ratio is 6.3 (Fig. 5). This is the widest known Type I lens.

The marginal scarps of the lenticular extension are quest-like; the northern scarp has a larger amplitude. The northern and southern walls of the trough are complicated by a series of terraces, which makes it possible to identify a younger lenticular formation within, 9.8 km wide with the same length (Fig. 5).

In the axial part of the lens, in the center, a small median ridge is interpreted, $\sim\!200$ m high, 4 km long, and $\sim\!2$ km wide. To the east and west of this ridge, long, narrow depressions 27 and 15 km in length have been recorded. The margins of the lenticular extension are bounded by intersects; nodal depressions have not been recorded.

Based on these data, it is possible to formulate a definition of lenticular extension, which refers to type I: a significantly deepened expansion of the active part of a transform fault, lenticular in plan view.

Lenticular extensions are usually associated with the maximum offset in the area of their discovery. Sizes in plan view vary from several tens to hundreds of kilometers. The marginal scarps are Cruciform; one scarp, as a rule, has a greater amplitude. The peaks of the lenticular extension coincide with intersects; nodal depressions have not formed. In the gravitational field, such structures correspond to an intense negative

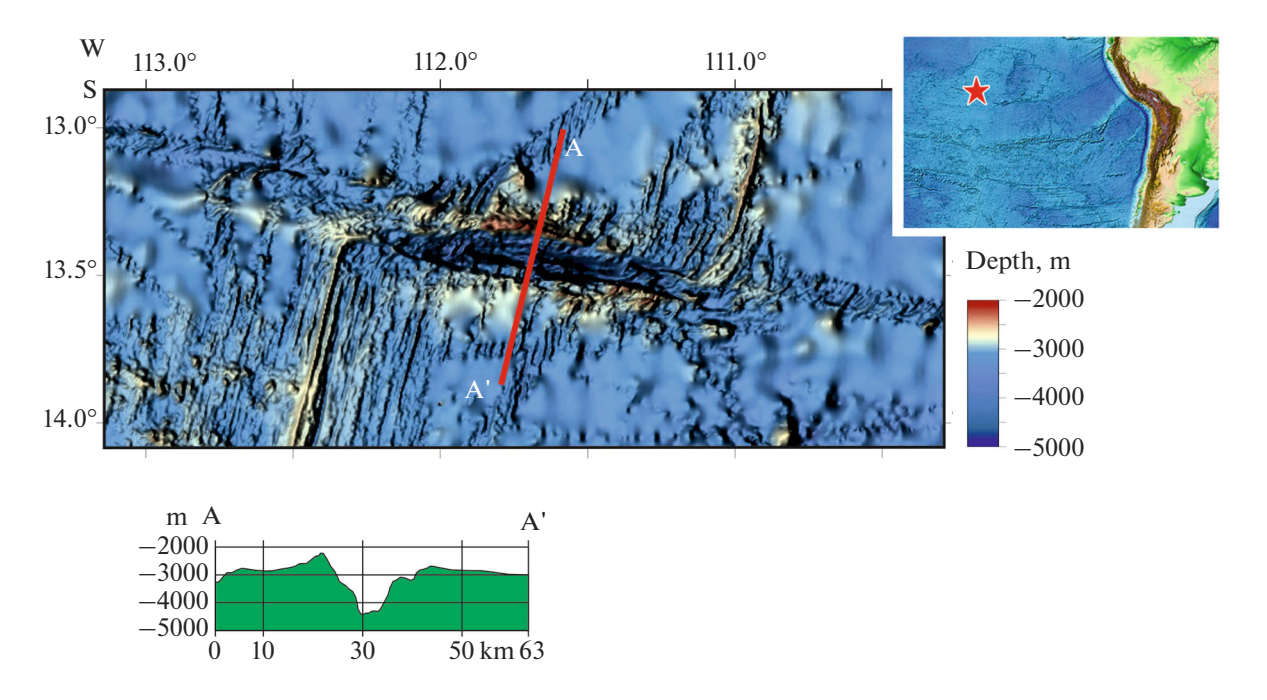


Fig. 5. Lenticular extension in active part of Garrett transform fault in Pacific Ocean(according to [35]). Transverse profile A–A' in central part of lenticular extension is shown. Inset: location of object (red asterisk).

anomaly Δg , lenticular in shape. These are young structural formations with an age not exceeding 10 Ma.

Lenticular Transformed Basin

For this type, we consider morphostructures representing the most complex lenticular formations of the global level, formed on large transform faults. The general characteristics of these structures are as follows

- lenticular shape;
- extreme offset:
- the presence of highly deformed lithosphere in the axial part of the lenticular block;
- the absence of internal axial faults and internal spreading zones.

Two such structures are located in the Equatorial Atlantic Ocean: the Vema transform fault and Romanche transform fault; and one in the Southwest Indian Ocean: the Andrew-Bain transform fault.

Vema transform fault. This fault is one of the largest in the Atlantic, with a total length of 3700 km and an offset length of ~ 310 km. The western flank can be traced for a distance of 1450 km; the eastern flank, for ~ 1940 km. On the gravity map, an intense negative anomaly corresponding to the Vema transform fault is clearly traced to the Antillean Arc in the west and is cut off by the Cape Verde Escarpment in the east.

In the area of the Vema transform fault, complex geological and geophysical expeditions were carried out, including GIN RAS cruises S19, S22, and S45

on the R/V *Akademik Nikolaj Strakhov* [3, 22, 25, 26, 28, 29, 31].

The lenticular extension formed in the Vema rift trough has a length of \sim 560 km, with a maximum width of 35 km in the area of the western intersect (Fig. 6a).

The transverse profile of the transform fault trough valley is U-shaped; the bottom is flat, and the depth is ~5 km. The Vema Trough is filled with an approximately 1-km-thick sediment layer.

In the axial part of the valley, in the western and eastern walls, the median ridge is clearly visible (Fig. 6a).

It is probably developed throughout the entire fault valley, but in the central part, it is hidden under a thick layer of sediments.

The walls of the lenticular extension are steep and quest-like, and the elevation above the valley floor is >1000 m (Fig. 6b).

On the southern side, a powerful transverse ridge has formed, the absolute height of which exceeds 3000 m with a length of \sim 320 km (Fig. 6b, profile B–B').

The minimum depth of the ridge part reaches 1033 m [32]. The ridge surface is flat with a thick (up to 500 m) carbonate structure comprising shallow lagoonal and/or reef limestones [22]. The transverse ridge underwent several stages of uplift and subsidence in an interval of 10-2 Ma [26]. In In the gravitational field, the ridge corresponds to an intense positive anomaly Δg (>100 mGal) (Fig. 6c).

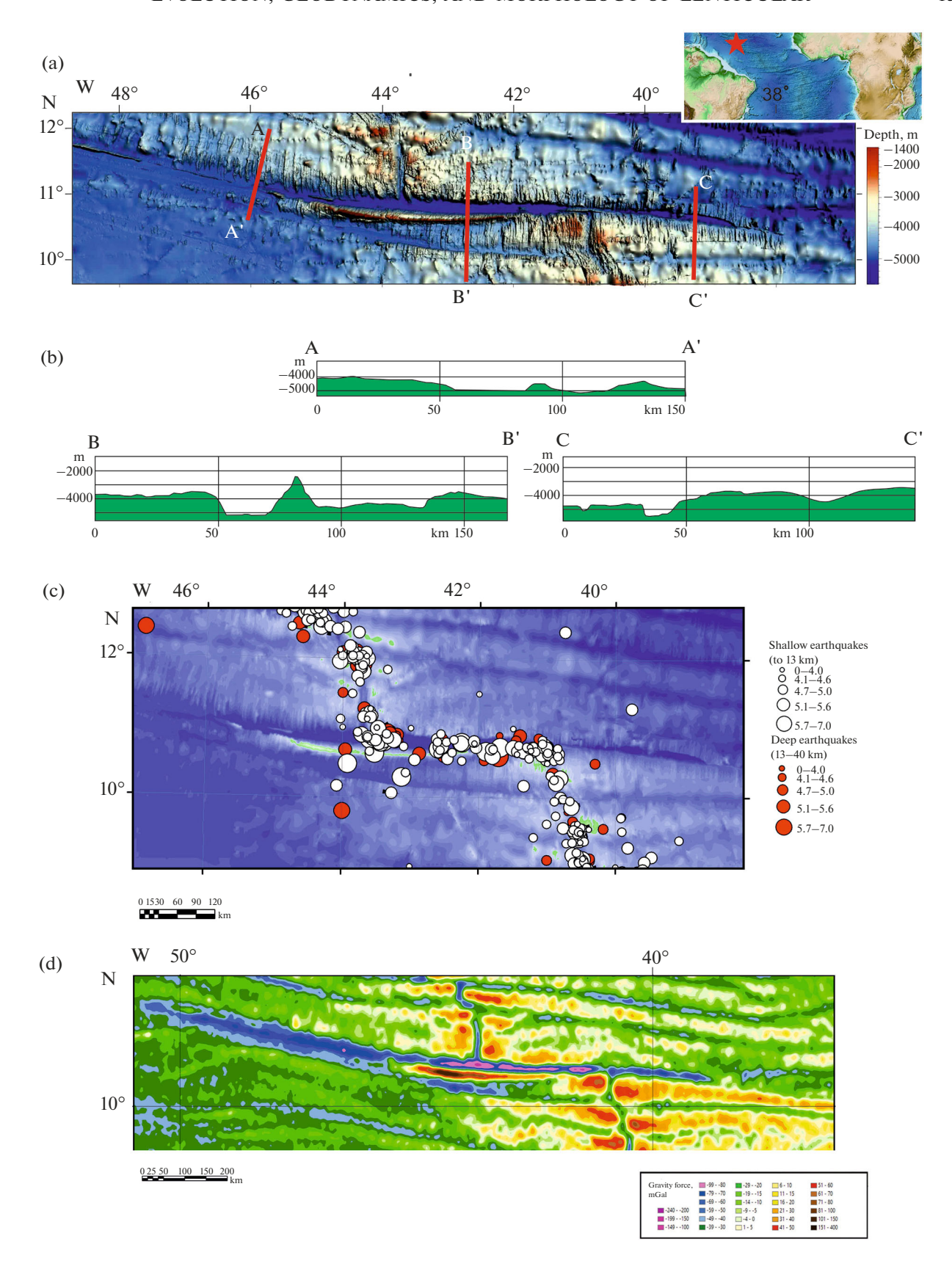


Fig. 6. Lenticular extension in active part of Vema transform fault in Atlantic Ocean. Inset: location of object (red asterisk). (a) Vema transform fault (according to [35]); (b), transverse profiles A-A', B-B', C-C' of relief; (c) seismicity map for events with magnitude M > 5 (according to [37]); (d) anomaly map Δg (according to [32]).

Seismic events of a strike-slip nature have been recorded along the northern margin of the fault valley (Fig. 6d).

Romanche transform fault. This is one of the longest faults in the Atlantic Ocean: the total length is 4300 km; the offset length is 880 km (Fig. 7a).

It is classified as a demarcation fault [5]. The western flank can be traced for a distance of 1600 km; the eastern flank, for 1800 km. The Romanche fault corresponds to an intense negative gravity anomaly (Fig. 7d). It is traced from South America to Africa and is consistent with the structural pattern of these continents.

The Romanche transform fault formed on the site of a large continental pre-rift shear zone and its age exceeds the age of the opening of the equatorial segment of the Atlantic [24].

In the active part of the fault, a lens of highly deformed lithosphere formed. On the western flank, the top of the lens rests against the MOR; on the eastern flank, the top is located outside the active part of the Romanche transform fault at a distance of ~150 km. The total length of the expansion lens is 1110 km, with a width of 88 km, the length-to-width ratio is 12.6. The rate of displacment of the flank is 32 mm/year, and the age of the lens is estimated at 55 Ma [27].

According to M. Ligi et al. [29], the active Romanche transform fault is a diffuse boundary between two segments of the central ridge. The displacement occurs along two arcuate faults, with the southern segment being more active. The lenticular zone itself consists of subparallel transverse ridges and valleys separating them [29].

From the north, the Romanche transform fault is bounded by a clearly defined in the relief by a quest-like boundary scarp (Figs. 7a, 7b, profile B–B').

The scarp is divided by transverse faults into separate blocks. In the western part, the absolute height of the escarpment is ~ 500 m; to the east, the escarpment turns into a clearly defined large transverse ridge, the relative height of which on the eastern flank reaches 2 km (Fig. 7b, profiles B–B', C–C').

To the south is a lenticular valley consisting of several fault troughs. In the eastern part of the valley, two depressions with a flat bottom (depth \sim 4300 m) filled with dislocated sedimentary rocks are clearly interpreted [27]. Further south beyond the valley lies a massive sublatitudinal ridge, complicated by a series of uplifts. This ridge joins the northern boundary scarp at its flanks, forming a single lenticular mountain structure with a relict valley sealed inside (Figs. 7a, 7b, profile A–A').

The western peak of the mountain structure abuts the western intersect. The eastern flank of the mountain structure extends far beyond the active part of the valley of the Romanche transform fault. The absolute height of the flanks significantly exceeds the height of the central part of the mountain structure.

From the south, this massive mountain structure is framed by the active trough of the Romanche transform fault, which is clearly visible in the relief. This is a lenticular, narrow depression, the bottom of which is complicated by a series of depressions and median ridges separating them. The sides of the Romanche trough are steep; in cross-section the valley resembles a graben (Fig. 7b, profile B—B'). The relative depth of the depression varies from 1.5 km (in the eastern flank) to 3.5 km (near the eastern intersect).

In the eastern part of the Romanche trough is one of the deepest basins of the Atlantic Ocean—the Vema Basin, which has a depth of 7856 m. The active fault trough Romanche, is an area of concentration powerful seismic manifestations (Fig. 7c).

In the west, the Romanche trough abuts the western intersect, while in the east it extends far beyond the active part of the transform fault. There are no nodal depressions in the Romanche transform fault.

The southern margin of the fault valley is represented by a clearly defined quest-like boundary scarp with a steep northern margin and a gentle southern margin. The scarp has an arcuate shape in plan view and is cut into separate blocks by submeridional grabenlike structures.

The lenticular transform basin formed in the trough of the Romanche transform fault is an ancient, multilevel structure that has experienced several stages of activation and relative quiescence during its history [29]. The transoceanic Romanche transform fault is characterized by spatiotemporal instability of geodynamic systems. Its different parts are characterized by different geological history [11]. It is likely that during periods of increased tectonic movement, either shear or extension processes across the main trough could have predominated, reflected in the complex structure of the relief [27, 29].

Andrew-Bain transform fault. This zone is located in the area where the African—Antarctic and West Indian segments of the mid-ocean ridge join. The fault marks an ancient transform fault separating the African—Arabian and Antarctic plates. The total length of the zone is >5500 km [9].

A lens of highly deformed lithosphere formed in the active part of the Andrew-Bain fault trough. The western peak of the lens coincides with the western intersect, the eastern peak extends 230 km beyond active zone. The total length of the lenticular extension reaches 818 km, with a maximum width of 105 km (Fig. 8a). The length-to-width ratio is 7.8.

From the northwest, the Andrew-Bain fault zone is abutted by a Cruciform boundary scarp expressed in relief (Figs. 8a, 8b, profiles A–A', B–B', C–C'). The height of the scarp above the bottom of the adjacent transform fault trough is \sim 3 km (on the southern flank) and decreases to 2 km (on the northern flank).

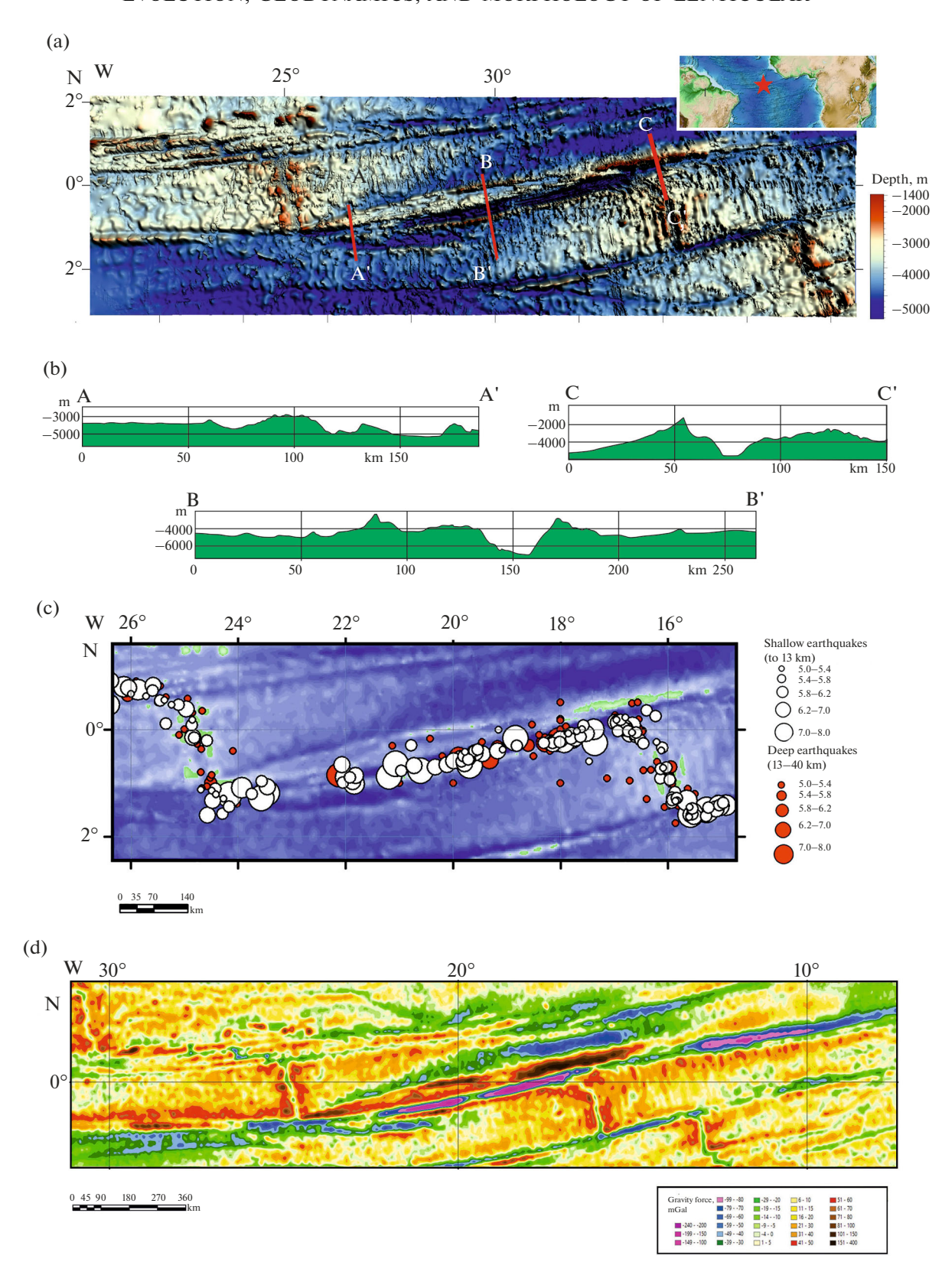


Fig. 7. Lenticular extension in active part of Romanche transform fault zone in Atlantic Ocean. Inset: location of object (red asterisk). (a) Romanche transform fault (according to [35]); (b) transverse profiles A-A', B-B', C-C' of relief; (c) seismicity map for events with magnitude M > 5 (according to [37]); (d) anomaly map Δg (according to data from [32]).

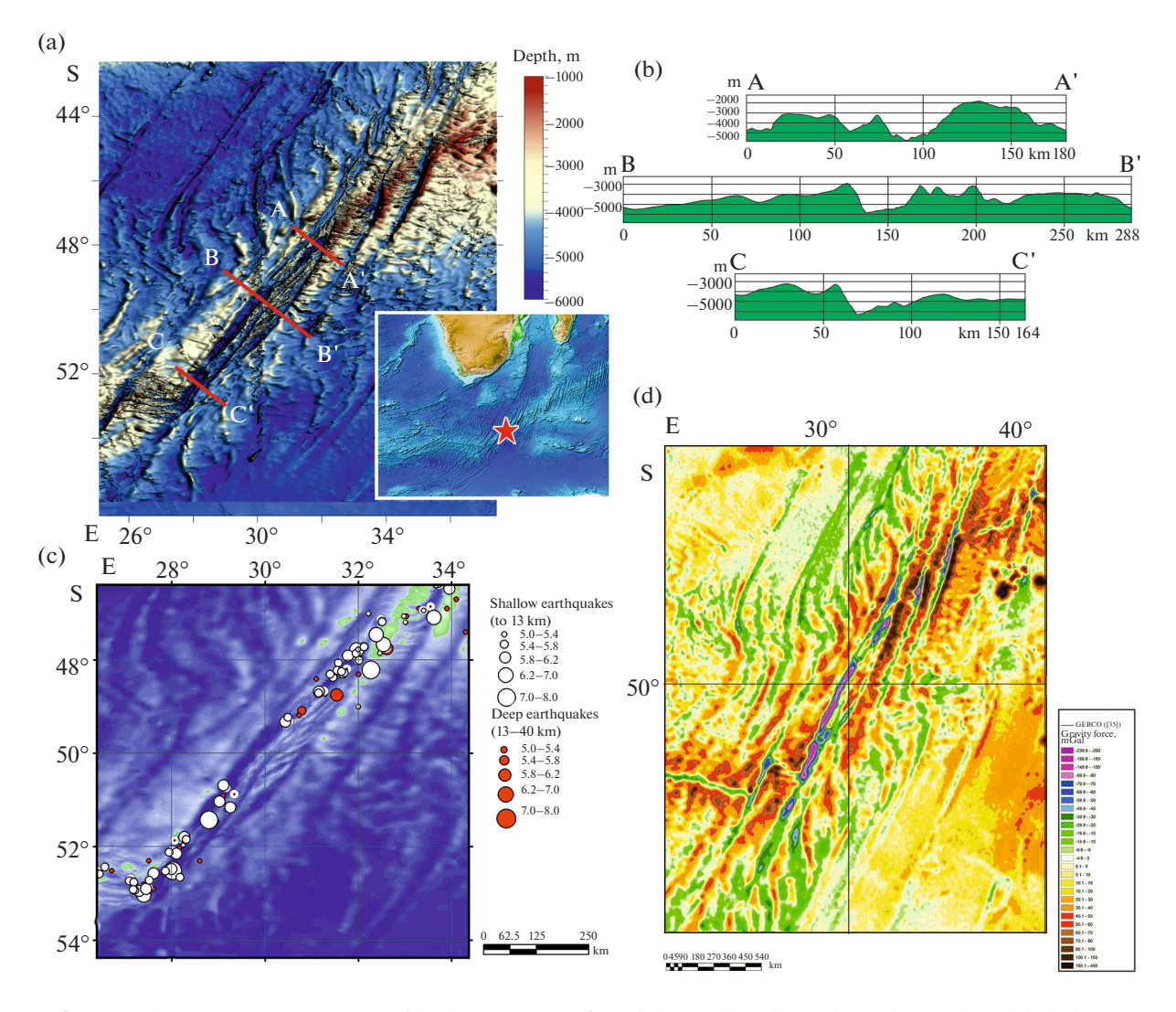


Fig. 8. Lenticular extension in active part of Andrew-Bain transform fault in Indian Ocean (according to [35]). (a) Andrew-Bain transform fault (according to [35]); (b) transverse profiles A-A', B-B', C-C' of relief; (c) seismicity map for events with magnitude M > 5 (according to [37]); (d) anomaly map Δg (according to data from [32]).

In the southern part of the Andrew-Bain zone, a transverse ridge is developed on the boundary scarp, the elevation of which above the bottom of the trench reaches 3500 m [8].

On the northern flank, the scarp is divided by transverse faults into separate blocks. A narrow, deep valley adjoins the scarp from the southeast. The valley reaches its maximum depth in the southern part (\sim 6300 m); to the north, the depth decreases and does not exceed 6000 m. The valley coincides with a bright negative anomaly in the gravity field (up to -100 mGal) (Fig. 8c).

The valley is ~ 20 km. The transverse profile is sharply asymmetrical with a steep and high northwestern slope (elevation ~ 3000 m) and a more gently dipping and low eastern slope (no more than 1000 m).

To the east of the valley there is a small ridge and a subparallel valley, which to the south turns into a len-

ticular zone. This area consists of a series of en echelon ridges, oriented at an angle of 30° to the general strike of the fault trough and forming a spindle-shaped pattern in plan view.

To the east is another narrow trough valley, bounded on the east by a quest-like scarp. In the southern part the scarp is represented several separate blocks. In the northern part, the scarp is a massive structure that merges with the arched uplift.

The central part of the lenticular transformed Andrew-Bain basin is characterized by positive gravity anomalies (30~50 mGal), which differ little from the background surrounding the transform fault (Fig. 8d).

A bright positive anomaly (>100 mGal) is recorded only on the marginal scarp in the area of the arch uplift near the northeastern intersect (Fig. 8d).

Earthquake epicenters gravitate mainly toward the northwestern valley, which indicates that the main shear movements are concentrated along the western boundary of the lenticular formation (Fig. 8c).

No transformed lenticular extensions have been identified in the Pacific Ocean.

Consequently, the lenticular transform basin is formed on the site of an ancient continental global strike-slip fault zone in areas with slow spreading, and the lenticular formation formed on a transform fault with an extreme offset for the region.

The complex morphology of the lenticular formation includes numerous second-order structural formations: curved troughs and intertrough ridges arranged in an en echelon manner, often forming a spindle-shaped pattern, but without signs of internal along-axial shear and spreading. Active shear processes are confined to one of the arcuate troughs that bound the lens.

One of the peaks of the lens extend far beyond the active part of the transform fault, the other peak is connected with the intersect. The marginal scarps are quest-like. The length of the lenticular formation significantly exceeds the offset of the parent fault and is several hundred and first thousand kilometers, the width reaches 150–250 km. In their history, these structures have experienced periods of activation and relative rest, which is reflected in their complex morphology.

Multitransform Lenticular System

In the case where the displacement along one of the bounding arcuate faults cannot compensate for the shear stresses, the lenticular extension can be transformed into a lenticular multitransform region with internal spreading zones. Its formation on the site of a single transform fault with a large offset is confirmed by the planned pattern of arcuate marginal scarps bounding the lens, the shape of the lens peaks and their transition to single-trough passive transform flanks, as well as the crowding of transform fault troughs inside the lens (Fig. 9).

Similar structures have been recorded in the Equatorial Atlantic (Doldrums and São Paulo) and in the southern Pacific Ocean (Valdivia). In the Indian Ocean, such structural formations have not been identified (Fig. 1).

The Doldrums multitransform lenticular system is located in the Central Atlantic near 7° – 8° N; this system includes (Fig. 9a):

- Doldrums fault;
- Vernadsky fault;
- northern and southern troughs of the Pushcharovsky fault;
 - Bogdanov fault.

The lens is bounded to the north and east by the Doldrums fault, while to the south and west the lens is bounded by an unnamed fault, which is located 50 km

south of the Bogdanov fault and is defined in the intersection zone with the mid-ocean ridge as nontransform displacement. The boundary faults have an arcuate shape in plan view, and their flanks cut off the flanks of the intratransform fault troughs. Distinctive feature The Doldrums multitransform lenticular system is an internal spreading zone with short spreading rift valleys and a high density of transform faults [15]. The total offset is approximately 630 km.

S.Yu. Sokolov et al. [19, 20] identified the Doldrums multitransform lenticular system as a separate class of polyfault systems.

S.G. Skolotnev et al. [15] refers this system to the megatransform class.

The zone has been almost completely covered by multibeam bathymetric surveys: integrated expeditions S06, S09, S22, and S45 were carried out here in 1987–2019 by GIN RAS on the R/V *Akademik Nikolaj Strakhov* [15, 16].

The length of the Doldrums multitransform lenticular system is ~ 1620 km, which is more than two times larger than the total offset of the transform faults included in the system. The width in the central part is 175 km. The length-to-width ratio is 9.3.

The peaks of the lens are far away beyond the total active part of the transform faults included in it:

- the western peak is located 500 km west of the Doldrums fault intersect;
- the eastern peak is located 530 km east of the Bogdanov fault intersect.

The Doldrums multitransform lenticular system can be divided into northern and southern parts.

The northern part has a lenticular shape and a width of up to 70 km, bounded from the north by the Doldrums transform fault and includes the Doldrums—Vernadsky intrafault region, which has a lenticular shape and a width of up to 50 km (Fig. 9a). From the south, the northern region is bounded by the Vernadsky transform fault. The parameters of the transform faults are as follows:

- the depth of the valley is 4700 m; the width, 14—19 km (Doldrums fault);
- the depth of the valley is 5000 m; the width, 5—10 km (Vernadsky fault).

Large median ridges have formed in the troughs. The relief of the spreading segment, which is part of the northern region and the intertrough block, is close to the classical morphology of the structures of the arch rise of the MOR.

To the south is a lenticular zone formed by closely spaced narrow deep transform fault valleys (width 4–8 km, depth >5000 m). The valleys are located at distances of 30, 15, and 30 km from each other.

Such a close location causes the formation of a unique relief in the intertrough space, where sigmoid ridges are located in the central uplift, between two

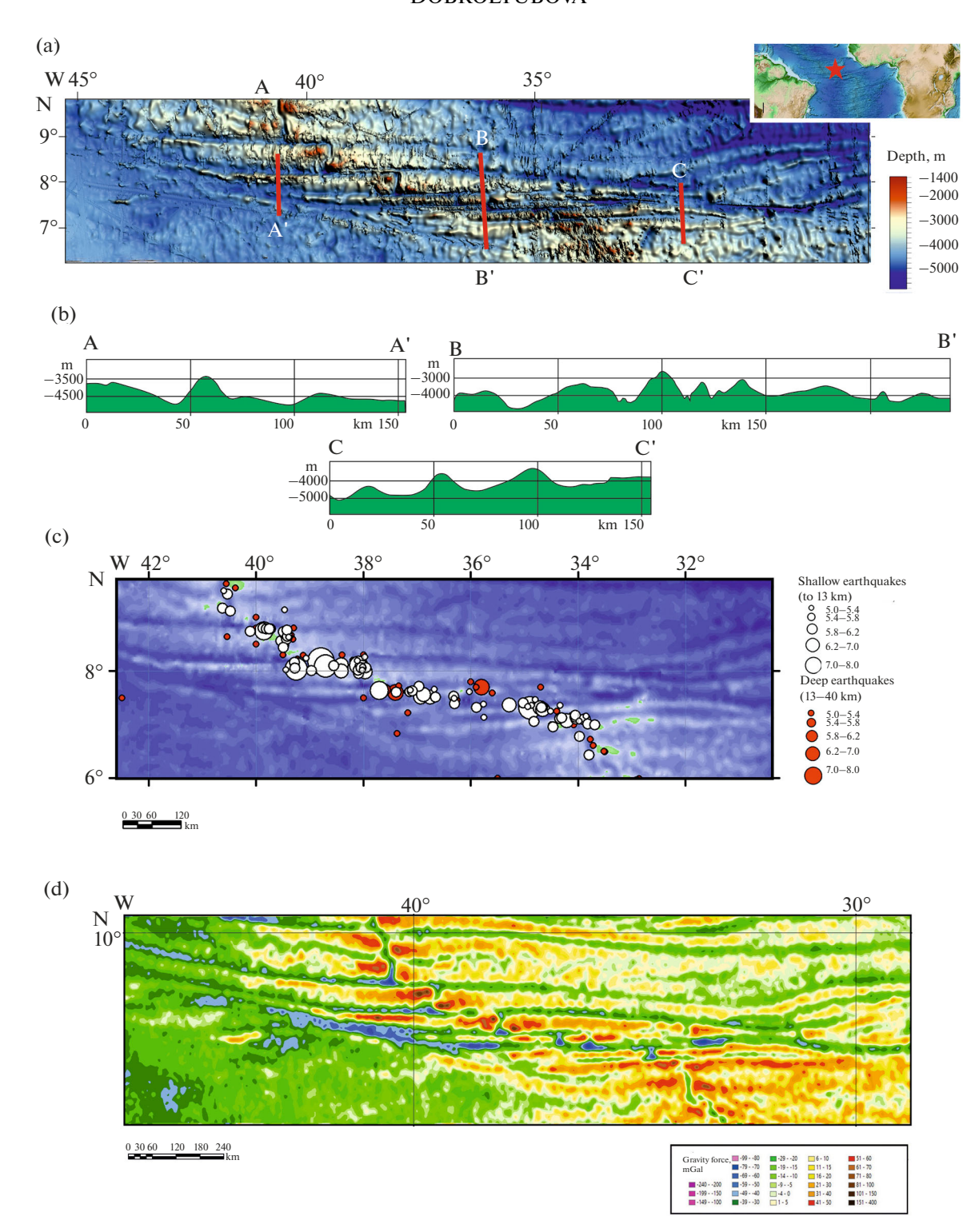


Fig. 9. Doldrums multitransform lenticular system in Atlantic Ocean. (a) Doldrums lenticular system (according to [35]); (b) transverse profiles A–A', B–B', C–C' of relief; (c) seismicity map for events with magnitude M > 5 (according to [37]); (d) anomaly map Δg (according to data from [32]).

troughs of the Pushcharovsky fault (the width does not exceed 15 km), and chains of block ridges in two wider intertrough areas, located north and south of the Pushcharovsky fault. The spreading segments making

up the Doldrums multitransform lenticular system are characterized by a morphology typical of the MOR with the formation of narrow deep rift valleys, nodal depressions, and angular scarps [15].

From the south and southwest, the multitransform lenticular Doldrums system is bounded by an arcuate scarp, divided into separate ridges. In the area of the rift uplift, the scarp turns into a nontransform offset at a latitude of $6^{\circ}47'$ N.

In the gravity field, the Doldrums multitransform lenticular system is clearly expressed, but without pronounced extrema (Fig. 9c). Negative values are associated with the active parts of transform faults and spreading segments. The eastern peak is characterized by values of about -10~mGal, but for the entire western flank of the lens, values of up to -50~mGal were recorded, which is typical of nodal depressions and troughs.

Seismic events are associated with transform faults and spreading segments located within the Doldrums multitransform lenticular system (Fig. 9d).

São Paulo multitransform lenticular system. This system is located in the equatorial Central Atlantic and includes four fault troughs connected by three small fragments of the MOR (Fig. 10a).

The total offset is about 560 km. The length of the lens is 1400 km, the width is 86 km; the length-to-width ratio is 16.3. The western flank extends beyond the MOR by 230 km, and the eastern flank, by 600 km (Fig. 10).

Thus, the lenticular structure is characterized by a clearly expressed eastern asymmetry.

Further on the flanks, beyond the lenticular zone, the transform fault can be traced to the west as a single trough and to the east as a double trough, all the way to the continental margins of Africa and South America, with a total length of ~3800 km [1]. Based on the time of its formation, the São Paulo transform fault is classified as a synrift structure [30].

A unique feature of the São Paulo multitransform lenticular system is not only the asymmetry of the flanks, but also the asymmetry of the location of the troughs of the MOR, confined to the eastern side of the active region of the lens. However, if we consider the lens as an independent object, then the location of the MOR troughs with respect to the lens peaks can be considered symmetrical. The origin of the lens is confined to the Eocene—Paleocene boundary [29]. It is likely that the restructuring of the entire region dates back to this time.

From the north-northeast and south-southwest, the São Paulo multitransform lenticular system is bounded by transform faults along which scarps have formed:

- northern (clear linear quest-like);
- southern (expressed in relief by chains of low, scattered ridges).

Intra transform fault troughs are located at intervals of \sim 30 km. The depth varies between 4000–4200 m. The width is 7–10 km. The passive parts of the troughs

are filled with sediments; in the active parts, small fragmentary median ridges have developed.

The transform faults are separated from each other by mountain structures, which are massive block uplifts, gradually turning into scattered narrow ridge ridges with a submeridional trend going away from the MOR. Near the extreme western intersect on the eastern (active) side, the northern boundary scarp is built up by a massive sublatitudinal mountain range (Atoba Ridge), ~100 km long and 25 km wide. The absolute height exceeds 3500 m. The summit surface of the ridge reaches the exposed surface and forms the island of St. Peter and Paul (Fig. 9a).

In the gravity field, the São Paulo multitransform lenticular system is expressed without major extrema. The absence of strong negative anomalies along the troughs indicates that the system does not have as insufficient a mass volume as the Romanche transform fault, 250 km to the south. Intersects and trough valleys are marked by negative anomalies. An intense positive anomaly (>100 mGal) is confined to the Atoba Ridge (Fig. 9d).

Most seismic events are concentrated within the active part of the lenticular system, with a maximum of events having a magnitude exceeding M > 6, confined to the northern trough. In the central part of the system, a zone of reduced seismicity is observed (Fig. 9c).

In the Pacific Ocean, in the Southern Hemisphere, one multitransform lenticular system that formed on the Valdivia fault system can be confidently identified, but there is no detailed bathymetric survey for this area, and in the morphostructural analysis, we used general coverage data [35, 37].

Valdivia multitransform lenticular system. This structure is located in the Southeast Pacific Ocean and includes seven fault troughs connected by six spreading segments.

The total offset is ~ 630 km. The length of the lens is 1850 km, and the width, 130 km; the length-to-width ratio is 14. The western flank extends beyond the MOR by 595 km; the eastern flank, by 610 km (Fig. 10a).

The valleys of transform faults, which bound the structure from the north-northwest and from the south-southeast, have a sublatitudinal strike over most of their length and only in the marginal parts do they change direction and cut off the flanks of the intratransform faults.

Intratransform faults have a sublatitudinal strike. The width of the valleys is 4-6 km, and the depth is $\sim 4600-4800$ m. The transform faults are separated from each other by mountain structures, which are massive block uplifts 20-25 km wide and up to 2000 m high, gradually turning into lower, scattered ridges with distance from the MOR.

Two troughs join at the eastern summit of the Valdivia multitransform lenticular system. The background

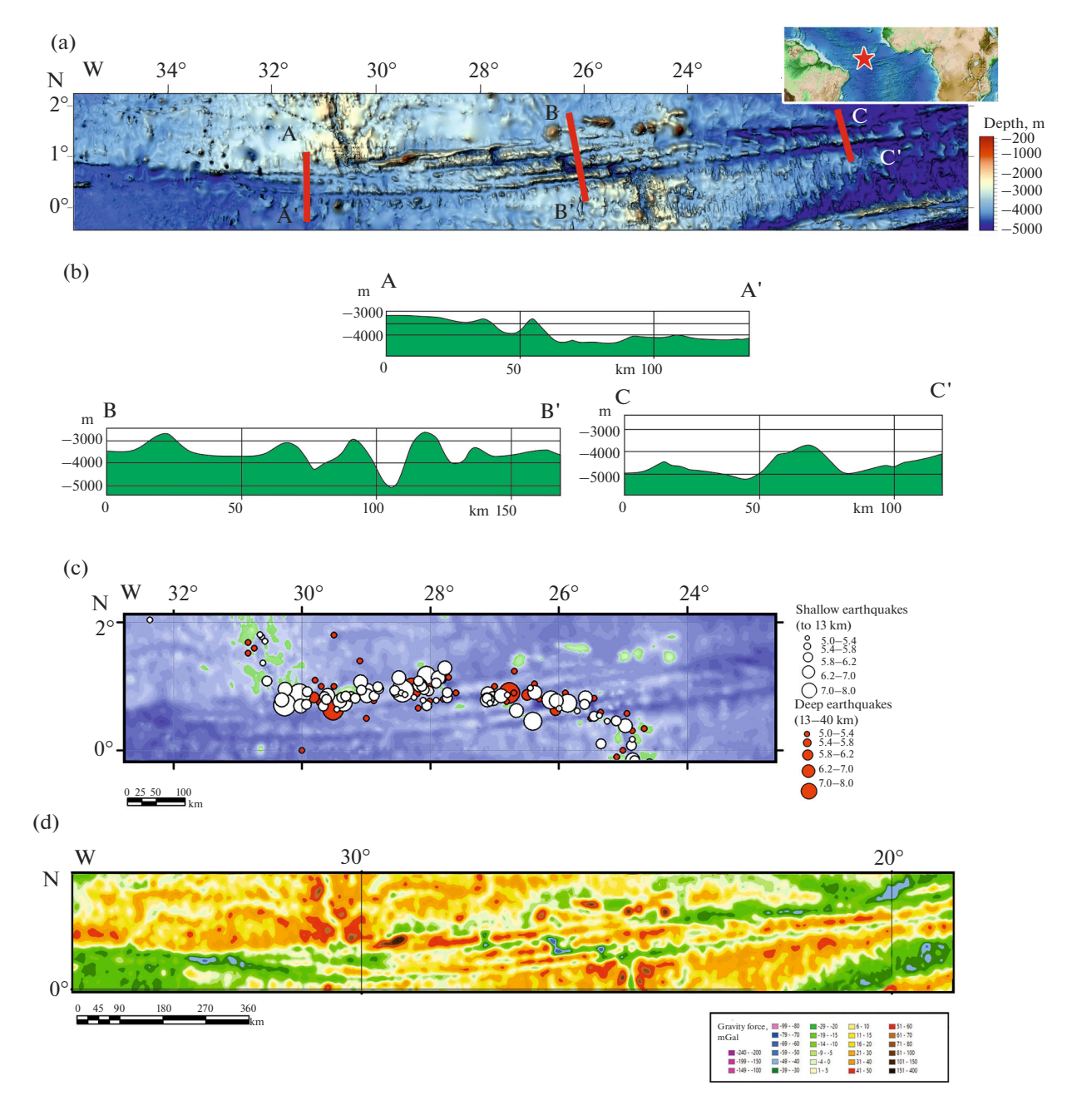


Fig. 10. São Paulo multitransform lenticular system in Atlantic Ocean. (a) São Paulo system (according to [35]); (b) transverse profiles A–A', B–B', C–C' of relief; (c) seismicity map for events with magnitude M > 5 (according to [37]); (d) anomaly map Δg (according to data from [32]).

depths are 3700 m, and the depth of the bottom of the trough valley reaches 5000 m.

In the west, near the western peak, the background depth is 4400 (north of the trough) and 4800 (south of the trough); the depth of the trough valley is 6300 m. Along the northern margin, a large narrow sublatitudinal mountain range has formed, 150 km long and 25 km wide. The height in the ridge part is \sim 3000 m. Further on the flanks, beyond the lenticular zone, the transform fault can be traced to the west and east as a single trough.

In the gravity field in the central and eastern parts of the multitransform lenticular system, the Valdivia multitransform lenticular system is clearly expressed, but without clearly defined extrema (Fig. 10d).

In the area of the western summit of the multitransform lenticular system, a maximum positive anomaly is observed, corresponding to a narrow ridge on the northern side of the trough (>100 mGal) and a significant negative anomaly in the trough valley (-80 to -99 mGal).

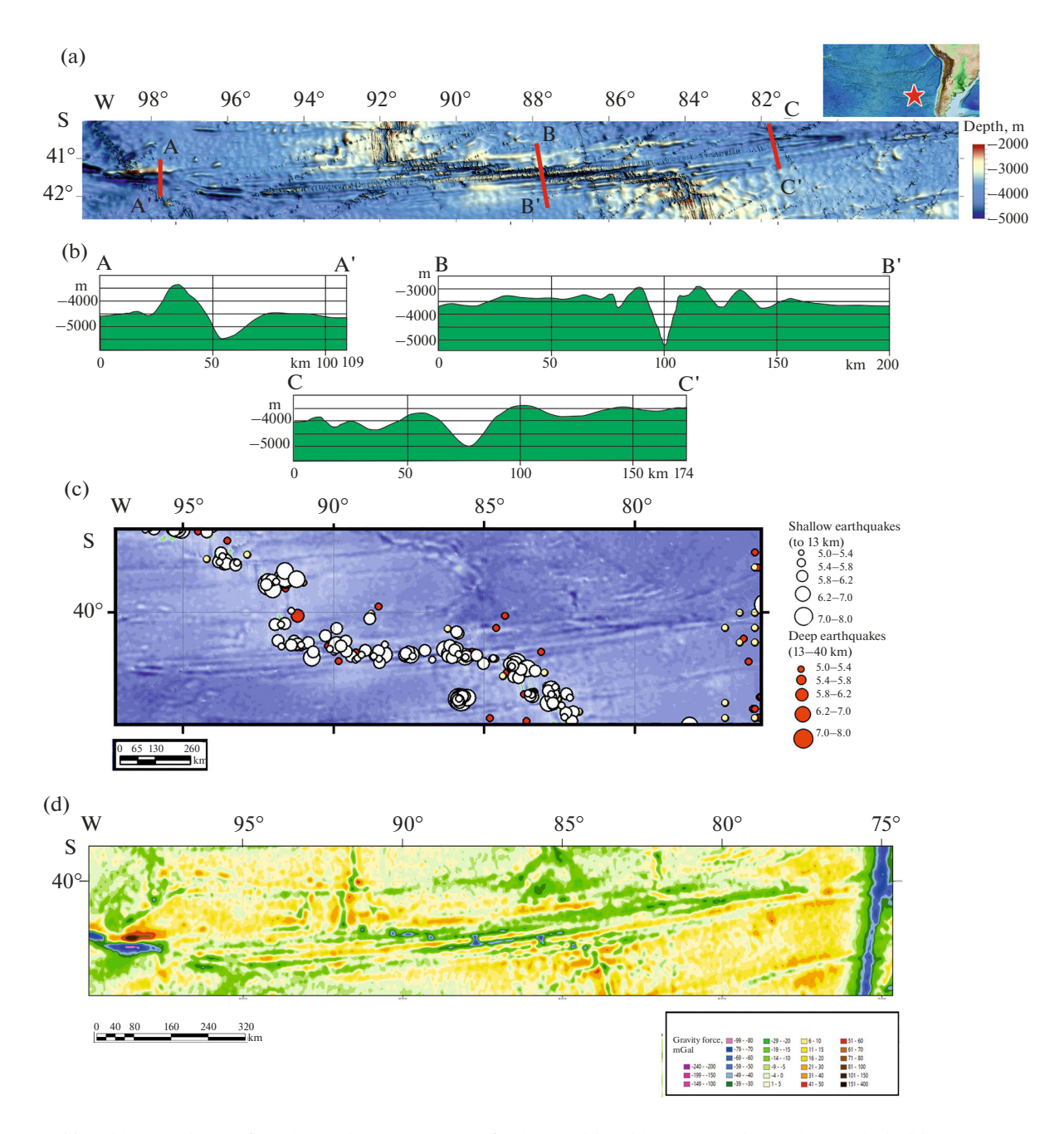


Fig. 11. Valdivia multitransform lenticular system in Pacific Ocean. (a) Valdivia system (according to [35]); (b) transverse profiles A–A', B–B', C–C' of relief; (c) seismicity map for events with magnitude M > 5 (according to [37]); (d) anomaly map Δg (according to data from [32]).

Seismic events are concentrated within the active parts of transform fault troughs and in spreading segments (Fig. 10c).

DISCUSSION

Geodynamic Interpretation

Lenticular extensions originate at transform boundaries in the active zone of a transform fault trough, in places with the thinnest oceanic crust, as a response to a global restructuring of the movement of lithospheric plates in the region when additional stretching occurs across the fault trough. Young lenticular extensions do not extend beyond the active region of the transform fault trough and mark the latest restructurings. The young formation looks like an overdeepened trough, which has a lenticular shape in plan view. Gradually, a median ridge and a single transform begin to form along the lens axis and splits into two arcuate troughs. The trough is divided into two arcuate troughs (Fig. 11).

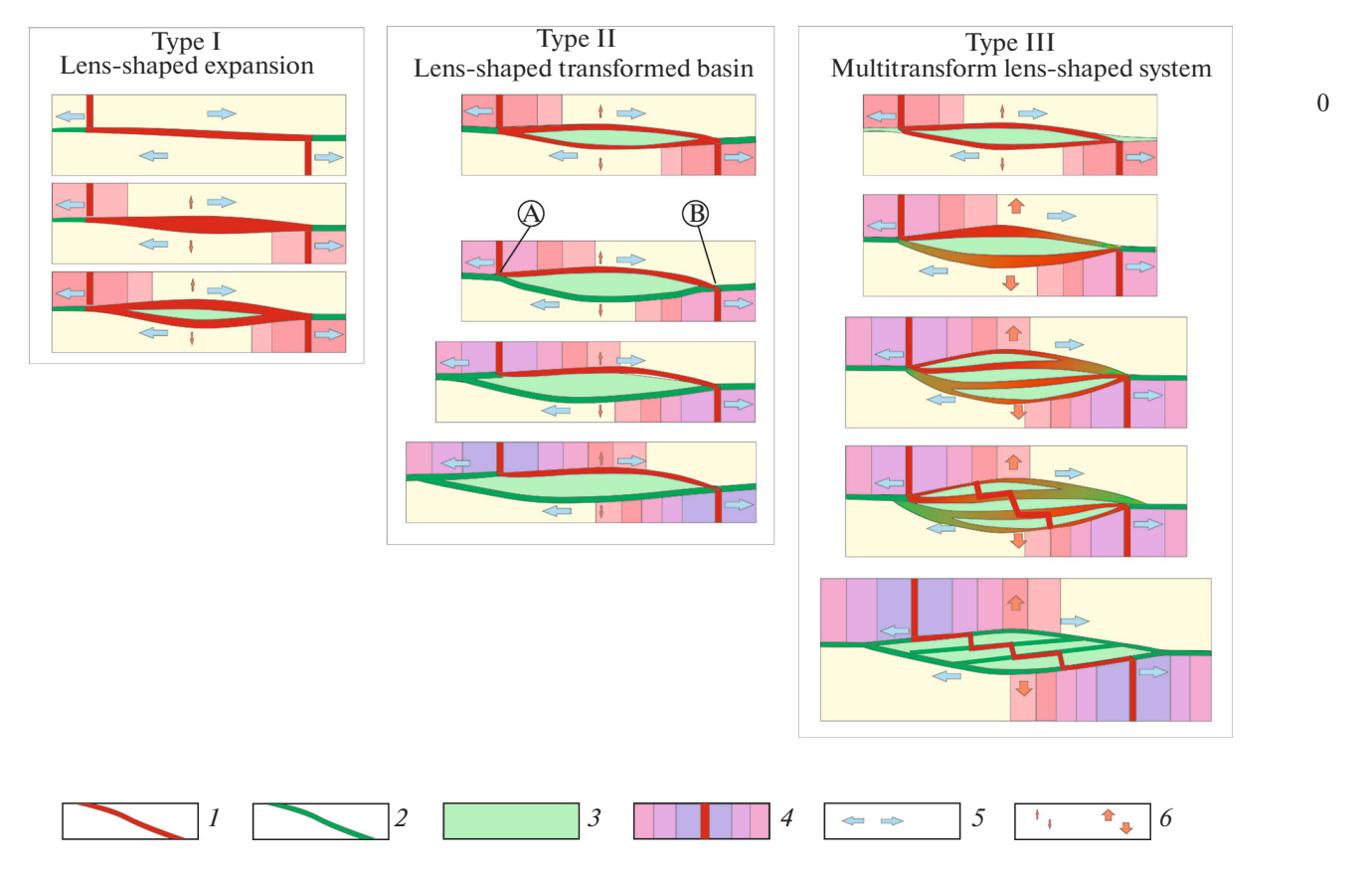


Fig. 12. Kinematic model of stages of opening and evolution of lenticular extensions in transform fault troughs: I-2, transform fault trough: I, active; I, passive; I, lens of highly deformed lithosphere; I, spreading ridge with newly formed portions of oceanic crust; I, spreading direction; I, stretching across transform fault trough, initiating opening of lenticular extension.

If the fluctuation in the direction of plate movement does not change, the lenticular extension begins to grow, extending beyond the active part of the transform fault. In this case, two scenarios are possible (Fig. 12):

- formation of a transformed lenticular basin, where shear stresses occur along one of the two framing troughs and growth proceeds toward one of the passive troughs;
- formation of a lenticular multitransform system with an internal spreading zone and lens growth in both directions along the host fault trough.
- In the first case (formation of a transformed lenticular basin), transform—accretionary structures develop. The mechanism appears to be as follows: in the inner region of the lenticular extension, a lens is formed, consisting mainly of exquoriented upper mantle rocks (dry spreading) subjected to intense tectonic impact [5].

Shear occurs along one of the two bounding troughs, which is confirmed by the obtained seismic data. This scenario occurs in the case when the spreading rate does not change for a long time or changes insignificantly and the system retains the ability to compensate for shear displacements without significant internal restructuring. The lens peaks are under different conditions.

One peak (adjacent) is formed where the active trough adjoins the Mid-Atlantic Ridge (Fig. 12).

Another peak (transverse), located in the area of the second intersect, where the active trough is opposite the intersection (Fig. 12).

The growth of the lenticular space due to accretion within its frame proceeds from the side of the adjacent lens peak towards the passive flank of the parent transform fault (Fig. 12).

• In the second case (formation of a lenticular multitransform system), accretion—spreading structures develop. This becomes possible when the displacement rate along the transform fault significantly exceeds the speed that was before the reconstruction, and the shift cannot be realized along one transform fault trough. At the initial stage, two arcuate framing faults remain active, and at later stages an internal system of troughs and spreading centers is formed (Fig. 12).

The system develops in such a way that in the axial part of the lenticular transform fault trough, a median ridge begins to form, then it grows and divides the transform valley into two troughs. Further, the median ridge develops into an interrift uplift and the lens begins to function as a system consisting of troughs, in which displacements occur realized along two bound-

ing troughs. The interrift uplift undergoes deformation, breaks up into several curved blocks, and expands. The bounding troughs begin to expand, acquire a lenticular shape, and median ridges begin to form in them, which gradually develop into interrift uplifts. Several subparallel troughs form inside the lens.

The intertrough uplifts are broken into blocks and internal spreading centers begin to form. Over time, the intense shifts along the intersecting troughs begin to fade, the lens peaks accrete to adjacent areas of the ocean floor, then begin to move with it towards the passive parts of the transform fault: the lenticular zone begins to grow due to internal spreading zones and extends far beyond the active part of the parent transform.

The growth of the lenticular zone across maternal transform faults with the formation of new transform fault troughs and spreading centers continues as long as there is transverse stretching and an increase in the divergence rate of continental plates in a given area.

With cessation of transverse stretching, the multitransform lenticular ceases to actively grow and continues to exist as a finely fragmented segment of the MOR. The lens peaks and framing scarps enter the oceanic plate and continue to passively move apart, while the transform fault troughs formed in the active region become parallel and the multitransform system changes from lenticular to almond-shaped.

CONCLUSIONS

- 1. Lenticular extensions form at transform boundaries where shear does not compensate for complex boundary interactions and they occur with the formation of complex multilevel transform, transform—accretion and transform—accretion—spreading structures.
- 2. The predominant confinement of lenticular extensions to the active segments of transform faults is explained by the fact that these are the the zones of greatest weakness, with thin crust and minimal magma flow, which are most susceptible to plate kinematic restructuring.
- 3. Lenticular extensions are found predominantly in the Southern Hemisphere, probably because lithospheric masses are moving in a northerly direction, and in the Southern Hemisphere there is a significant background with a submeridional extension component and spreading cannot fully compensate for the newly formed space.
- 4. The author has highlighted three types of active lenticular extensions:
 - lenticular zone;
 - transformed lenticular basin;
 - multitransform lenticular system.
- 5. All lenticular extensions are characterized by the presence of specific quest-like margin scarps that can be used in paleogeographical reconstructions, since

they are the key structural element marking geodynamic restructurings in the World Ocean.

ACKNOWLEDGMENTS

The author thanks her colleagues for their help and support, and the crew of the R/V Akademik Nikolaj Strakhov for their professionalism and dedicated work in the difficult expeditionary conditions of the Atlantic Ocean. The author is grateful to reviewers A. A Mazarovich (GIN RAS, Moscow, Russia) and A A Peyve (GIN RAS, Moscow, Russia) for helpful comments and to editor M N. Shoupletsova (GIN RAS, Moscow, Russia) for careful editing.

FUNDING

The study was supported by Russian Science Foundation, project no. 24-17-00097 "Atlantic—Arctic Rift System: Segmentation, Evolution, Structure Formation, and Modern Geodynamics."

CONFLICT OF INTEREST

The author of the work declares that she has no conflicts of interest.

REFERENCES

- 1. G. V. Agapova, "The features of the morphology of the San-Paulo Fracture Zone (equatorial Atlantic)," Okeanologiya **34** (1), 107–112 (1994).
- 2. E. P. Dubinin, *Transform Faults in the Oceanic Lithosphere*, Ed. by S. A. Ushakov (Mosk. Gos. Univ., Moscow, 1987) [in Russian].
- E. V. Ivanova, S. G. Skolotnev, D. G. Borisov, A. N. Demidov, A. S. Bich, F. N. Gippius, A. S. Gryaznova, K. O. Dobroliubova, T. F. Zinger, D. M. Korshunov, O. V. Levchenko, V. V. Mashura, F. Muccini, N. V. Nemchenko, A. A. Peyve, A. N. Pertsev, K. Sani, A. Sanfilippo, N. V. Simagin, S. Yu. Sokolov, C. Ferrando, N. P. Chamov, I. B. Shakhovskoy, and K. N. Sholukhov, "Multidisciplinary investigation of the transform fault Zzones Doldrums and Vema during cruise 45 of the R/V "Akademik Nikolaj Strakhov"," Oceanology 60, 424–426 (2020).
 - https://doi.org/10.31857/S0030157420030028
- A. O. Mazarovich, G. V. Agapova, V. N. Efimov, M. Ligi, S. Yu. Sokolov, N. N. Turko, and A. A. Rikhter, "Passive parts of fracture zones in the Atlantic Ocean between 16° N and the equator," Geotectonics 31 (5), 420–429 (1997).
- 5. A. O. Mazarovich, Geological Structure of Central Atlantic: Fracture Zones, Volcanic Edifices and Deformations of the Ocean Floor, Ed. by Yu. G. Leonov (Nauchn. Mir, Moscow, 2000) [in Russian].
- A. O. Mazarovich, K. O. Dobrolyubova, V. N. Efimov, S. Yu. Sokolov, and N. N. Turko, "Topography and deformation of oceanic crust south of the Cape Verde Islands, Atlantic Ocean," Dokl. Earth Sci. 379 (6), 615– 619 (2001).

- A. A. Peive, "Vertical tectonic movements of the crust in transform fracture zones of the Central Atlantic," Geotectonics 40, 25–36 (2006).
- A. A. Peyve, S. G. Skolotnev, M. Ligi, N. N. Turko, E. Bonatti, S. Yu. Kolodyazhnyi, N. P. Chamov, N. V. Tsukanov, Yu. E. Baramykov, A. E. Eskin, N. Grindlay, J. Sklater, D. Brunelli, A. N. Pertsev, A. Cipriani, J. Bortoluzzi, R. Mercuri, E. Paganelli, F. Muchini, Ch. Takeuchi, F. Zafagninni, and K. O. Dobrolyubova, "Investigation of the Andrew Bain transform fault zone (African-Antarctic region)," Dokl. Earth Sci. 416 (1), 991–994 (2007).
- A. A. Peyve, "Accretion of oceanic crust under conditions of oblique spreading," Geotectonics 43, 87–99 (2009).
- 10. Yu. M. Pushcharovsky, Yu. N. Raznitsin, and A. O. Mazarovich, *Structure of the Doldrums Fracture Zone: Central Atlantic* (Nauka, Moscow, 1991) [in Russian].
- 11. Yu. M. Pushcharovsky, A. A. Peyve, A. S. Perfil'ev, Yu. N. Raznitsin, and N. N. Turko, "Tectonics of the Romanche Fracture Zone, equatorial Atlantic," Dokl. Akad. Nauk SSSR **334** (1), 77–79 (1994).
- Yu. M. Pushcharovskii, A. A. Peive, Yu. N. Raznitsin, and E. S. Bazilevskaya, *Rift Zones of Central Atlantic* (GEOS, Moscow, 1995).
- S. G. Skolotnev, N. N. Turko, S. Yu. Sokolov, A. A. Peive, N. V. Tsukanov, S. Yu. Kolodyazhnyi, N. P. Chamov, Yu. E. Baramykov, A. S. Ponomarev, V. N. Efimov, A. E. Eskin, V. V. Petrova, L. A. Golovina, V. Yu. Lavrushin, E. A. Letyagina, E. P. Shevchenko, K. V. Krivosheya, and L. V. Zotov, "New data on the geological structure of the junction of the Cape Verde Rise, Cape Verde Abyssal Basin, and Bathymetrists Seamounts (Central Atlantic Ocean)," Dokl. Earth Sci. 416 (7), 1037–1041 (2007).
- 14. S. G. Skolotnev, A. A. Peyve, N. N. Turko, M. E. Bylinskaya, and L. A. Golovina, "Accretion of crust in the axial zone of the Mid-Atlantic Ridge south of the Martin Vas Fracture Zone, South Atlantic," Geotectonics 43, 358–378 (2009).
- S. G. Skolotnev, K. O. Dobrolyubova, A. A. Peive, S. Yu. Sokolov, N. P. Chamov, and M. Ligi, "Structure of spreading segments of the Mid-Atlantic Ridge between the Arkhangelsky and Bogdanov transform faults, Equatorial Atlantic," Geotectonics, No. 1, 1–20 (2022).
 - https://doi.org/10.31857/S0016853X22010088
- S. G. Skolotnev, A. Sanfilippo, A. A. Peive, F. Muccini, S. Yu. Sokolov, C. Sani, K. O. Dobroliubova, C. Ferrando, N. P. Chamov, A. N. Pertsev, A. S. Gryaznova, K. N. Sholukhov, and A. S. Bich, "New data on the structure of the megatransform system of the Doldrums (Central Atlantic)," Dokl. Earth Sci. 491 (1), 131–134 (2020). https://doi.org/10.31857/ S2686739720030184
- 17. S. Yu. Sokolov, "The state of geodynamical mobility in the the mantle from seismic tomography and ratios between velocities of P- and S-waves," Vestn. KRAUNTs.
- Nauki Zemle, No. 2, 55–67 (2014). 18. S. Yu. Sokolov, "Tectonic regularities of the mid-At-

lantic Ridge based on data on correlation between sur-

- face parameters and geodynamic state of the upper mantle," Vestn. KRAUNTs. Nauki Zemle **32** (4), 88–105 (2016).
- S. Yu. Sokolov, Yu. A. Zaraiskaya, A. O. Mazarovich, V. N. Efimov, and N. S. Sokolov, "Spatial instability of the rift in the St. Paul multifault transform fracture system, Atlantic Ocean," Geotectonics 50, 223–237 (2016). https://doi.org/10.7868/S0016853X16030115
- 20. S. Yu. Sokolov, "The tectonics and geodynamics of the Equatorial Atlantic," in *Transactions of Geological Institute of Russian Academy of Sciences*, Vol. 618), Ed. by K. E. Degtyarev (Nauchn. Mir, Moscow, 2018) [in Russian].
- 21. A. V. Tevelev, *Shear Tectonics*, Ed. by Al. V. Tevelev (Mosk. Gos. Univ., Moscow, 2005) [in Russian].
- 22. N. P. Chamov, S. Yu. Sokolov, and S. I. Merenkova, "Residual sediments of the Vema Fracture Zone, Central Atlantic," Lithol. Miner. Resour. 55, pp. 338–344. https://doi.org/10.31857/S0024497X2005002X
- 23. D. L. Anderson, T. Tanimoto, and Y. Zhang, "Plate tectonics and hotspots: The third dimension," Science **256**, 1645–1651 (1992).
- 24. K. Attoh, L. Brown, J. Guo, and J. Heanlein, "Seismic stratigraphic record of transpression and uplift on the Romanche transform margin, offshore Ghana," Tectonophysics, No. 378, 1–16 (2004). https://doi.org/10.1016/j.tecto.2003.09.026
- 25. E. Bonatti, R. Sartori, and A. Boersma, "Vertical crustal movements at the Vema fracture zone in the Atlantic: Evidence from dredged limestones," Tectonophysics, No. 91, 213–232 (1983).
- 26. E. Bonatti, M. Ligi, L. Gasperini, and E. Vera, "Imaging crustal uplift, emersion and subsidence at the Vema fracture zone," EOS Trans. AGU 75 (32), 371–371 (1994).
- 27. E. Bonatti, M. Ligi, L. Gasperini, A. Peyve, Y. Raznitsin, and Y. J. Chen, "Transform migration and vertical tectonics at the Romanche fracture zone, Equatorial Atlantic," J. Geophys. Res. **99**, 21 779–802 (1994).
- 28. E. Bonatti, D. Brunelli, W. R. Buck, and M. Ligi, "Flexural uplift of a lithospheric slab near the Vema transform (Central Atlantic): Timing and mechanism," Earth Planet. Sci. Lett. **240**, 642–655 (2005). https://doi.org/10.1016/j.epsl.2005.10.010
- 29. M. Ligi, E. Bonatti, L. Gasperini, and A. N. B. Poliakov, "Oceanic broad multifault transform plate boundaries," Geology **30**, 11–14 (2002). https://doi.org/10.1130/0091-7613(2002)030<0011:OBM-TPB>2.0.CO;2
- M. Marcia, S. Sichel, A. Briais, D. Brunelli, M. Ligi, N. Ferreira, T. Campos, B. Mougel, I. Brehme, C. Hémond, A. Motoki, D. Moura, C. Scalabrin, I. Pessanha, E. Alves, A. Ayres, and P. Oliveira, "Extreme mantle uplift and exhumation along a transpressive transform fault," Nat. Geosci. 621 (2016). https://doi.org/10.1038/ngeo2759
- 31. E. G. Morozov, A. N. Demidov, R. Y. Tarakanov, and W. Zenk, *Abyssal Channels in the Atlantic Ocean* (Springer, Library of Congress, New York, 2010, No. 2010934296). https://doi.org/10.1007/978-90-481-9358-5

- 32. E. Peyve, D. Bonatt, A. Brunelli, A. Chilikov, K. Cipriani, K. Dobrolubova, V. Efimov, S. Erofeev, V. Ferrante, L. Gasperini, R. Hekinian, M. Ligi, G. Maurizio, A. Mazarovich, A. Perfiliev, Y. Raznitsin, G. Savelieva, B. Sichler, V. Simonov, S. Skolotnev, S. Sokolov, and N. Turko, "New data on some major MAR structures: Initial results of the R/V Akademik Nikolai Strakhov 22 Cruise," InterRidge News 9 (2), (2000).
- 33. D. T. Sandwell and W. H. F. Smith, "Global marine gravity from retracked Geosat and ERS-1 altimetry: Ridge segmentation versus spreading rate," J. Geophys. Res. **114** (B1), 1–18 (2009).
- 34. Y. S. Zhang and T. Tanimoto, "Ridges, hotspots and their interaction, as observed in seismic velocity maps," Nature **355** (6355), 45–49 (1992).
- 35. GEBCO 30" Bathymetry Grid. Vers. 20141103, 2014. https://www.gebco.net. Accessed October, 2024.
- 36. GPS Time Series Data. 2022. Jet Propulsion Laboratory of California Institute of Technology. https://side-

- show.jpl.nasa.gov/post/series.html. Accessed October, 2024.
- 37. USGS Search Earthquake Catalog. 2022. https://earthquake.usgs.gov/earthquakes/search. Accessed November 17, 2022.
- 38. NASA. Bathymetric Data Viewer. https://www.nc-ei.noaa.gov/maps/bathymetry. Accessed October, 2024.
- 39. Golden Software Surfer. 2019. https://www.goldensoft-ware.com/products/surfer/. Accessed October, 2024.
- 40. Global Mapper. 2014. https://www.bluemarble-geo.com/global-mapper/. Accessed October, 2024.
- 41. ESRI ArcGIS. 2017. https://www.arcgis.com/index.htm. Accessed October, 2024.

Publisher's Note. Pleiades Publishing remains neutral with regard to jurisdictional claims in published maps and institutional affiliations. AI tools may have been used in the translation or editing of this article.